2021 43rd Annual International Conference of the
IEEE Engineering in Medicine & Biology Society (EMBC)
Oct 31 - Nov 4, 2021. Virtual Conference

Image reconstruction for the rotating RF coil using k-t bin robust principal component analysis (RPCA) method*

Ke Shi, Mingyan Li, Ewald Weber, Stuart Crozier, *Member, IEEE* and Feng Liu

***Abstract*—The recently developed rotating radiofrequency coil (RRFC) technique has been proven to be an alternative solution to phased-array coils for magnetic resonance imaging (MRI). However, most of the image reconstruction methods for the RRFC requires detailed knowledge of coil sensitivity to yield optimal results. In this work, a novel reconstruction algorithm based on Robust Principal Component Analysis (RPCA) with the k-t (k-space-time domain) sparse bin reformation method (or rotating k-t bin method) has been presented to restore images without using dedicated coil sensitivity information. The proposed algorithm recovers images by iteratively removing the artefacts in both temporal and frequency domains caused by the Fourier invariant violation from coil rotation. The data sampling scheme consists of the golden angle (GA) radial k-space and the stepping-mode coil rotation. Simulation results demonstrate the effectiveness of the proposed imaging method for the RRFC-based MR scan.**

I. Introduction

Magnetic resonance imaging (MRI) has been driven toward ultra-high magnetic fields (UHF, ≥7T) to gain the benefits of high signal-to-noise ratio (SNR), spatial resolution and image contrast accordingly. Due to the absence of a whole-body coil at 7T, the transceiver array coils are typically used for signal transmission and reception. During the transmit phase, the array coils utilize the parallel transmission (pTx) technology for the reduction of the field inhomogeneity and the specific absorption rate (SAR). During the reception, the SNR can be boosted by the array coils and the shortened acquisition time with fast imaging technologies, such as parallel imaging [1], simultaneous multi-slice [2], and compressed sensing [3]. However, expensive amplifier and array coils are essential to realize these advantages. Therefore, alternative solutions were investigated to enable the parallel MRI technology on those relatively lower cost single-channel systems.

Both parallel imaging and parallel transmit can benefit from the use of more coil elements. However, with a conventional stationary coil array, the coil number is limited by the space to accommodate more coils. On the other hand, the rotating MR coil can theoretically have more distinct sensitivity profiles by the coil rotation, which could reduce the scan time. Similarly, the pTx performance also relies on the number of the channels; the physical rotation can also bring extra spatial degree-of-freedom for the transmit sensitivity profile (B_1^+) shimming and SAR control [3, 4]. Hence, the single-channel rotating radiofrequency coil (RRFC) [5] and rotating radiofrequency coil array (RRFCA) [6] are designed to benefit both parallel imaging and pTx technologies by offering better safety control and B_1^+ shimming capability; leading to a better solution over the conventional RF coils.

In the past few years, several rotating MR image reconstruction algorithms have been developed, like the Time Division Multiplexed-Sensitivity Encoding (TDM-SENSE) method [4] radial trajectory with sensitivity averaging method [6] and the Sensitivity Self-Calibration with Eigen-decomposition approach method [7]. However, for the UHF MRI, the rotating coil receive sensitivity profile (B_1^-) varies at each distinct coil position, and accurate coil sensitivity estimations shall be acquired; otherwise, the motion artefacts caused by coil rotation can contaminate the images. Conventional sensitivity mapping methods are not applicable to the RRFC [7], thus challenges remain with the existing rotating MR imaging methods in the reconstruction for the human-sized objects.

Robust Principal Component Analysis (RPCA) [9] is a method that can achieve efficient suppression for noise and artefact; therefore, it is a perfect candidate to remove the motion artefacts for the image reconstruction of the RRFC. In this paper, we investigated the feasibility of using the RPCA for the image reconstruction of the rotating techniques, including a single-coil RRFC and a 4-element RRFCA.

II. Method

A. Robust Principal Component Analysis

A randomized k-space encoding scheme, as proposed in the k-t sparse [9] method, offers a high acceleration rate in dynamic MRI since those MR images are highly redundant in space and time domains. The sampled k-space data in the RRFC system has similar features with respect to the correspondence between phase encoding and its sampling angular positions. Here, we attempt to reconstruct images collected by the rotating coil using the k-t sparse strategy.

Robust principal component analysis (RPCA) is a mathematical method to reconstruct the unknown system matrix with the superposition of low-rank matrix (L) plus sparse matrix (S) components, where L can be modelled as

*Research supported by Australia Research Council Linkage Projects, Grant/Award Number: LP120200375

K. S. Author is with the Faculty of Information Technology and Electrical Engineering, St Lucia, QLD 4072 Australia (e-mail: ke.shi@uqconnect.edu.au)

M. L. Author is with the Faculty of Information Technology and Electrical Engineering, St Lucia, QLD 4072 Australia (email mingyan@itee.uq.edu.au).

E. W. Author is with the Faculty of Information Technology and Electrical Engineering, St Lucia, QLD 4072 Australia (e-mail: ewald@itee.uq.edu.au).

S. C. Author is with the Faculty of Information Technology and Electrical Engineering, St Lucia, QLD 4072 Australia (struart@itee.uq.edu.au).

F. L. Author is with the Faculty of Information Technology and Electrical Engineering, St Lucia, QLD 4072 Australia (corresponding author, phone: 61-07-3365-3982; feng@itee.uq.edu.au).

the slow-changing, highly-correlated background image and S can be represented as the highly dynamic components capture the rapidly changing information. Here we assume that the incoherence exists among spatial, frequency and temporal domain (or k-t space) with either L or S, the exact solutions of the low-rank and sparse components can be obtained by solving the regularization problem. The nuclear norm ℓ_* enforcement with the singular value soft thresholding will be implemented for temporal reconstruction, and the $\ell 1$ norm enforcement with the soft, sparse thresholding will be explored in the frequency domain [9].

The image reconstruction of the rotating MRI can be represented as the following optimization problem:

$$\begin{cases} \arg\min \frac{1}{2}\|EX-d\|_2^2+\lambda_L\|L\|_*+\lambda_s\|TS\|_1 \\ s.t \quad L+S=X \end{cases} \tag{1}$$

where d is the sampled k-space data K, L are the low-rank matrix, S is the sparse matrix, T is the unitary sparse transform operator like discrete Fourier transform, X is the superposition of L and X, λ_L and λ_S are the threshold parameters correspond to the $\|L\|_*$ and $\|TS\|_1$ matrices norm constraint terms. The data acquisition operator E includes the Fourier Transform and transceiver sensitivity.

B. k-t bin method

The k-space data acquired with the single-channel RRFC has sufficient spatial coverage of the subject by encoding various sensitivity profiles [10] around the subject. In practice, the k-space acquisition employs the golden angle radial sampling technique and the stepping mode with linear, angular increment as the coil rotation mechanism.

The k-t bin matrix $\tilde{d}$ can be reconstructed from k-space data acquired from the multiple sampling positions as follows:

k-t bin construction scheme

1. Assuming a 2D k-space $K \in \mathbb{C}^{Nx\times Ny}$ with the fully-sampled condition of $Ny = ceiling(\pi Nx/2)$. Scanning positions are denoted as $coil_n$ for $n=1,...,p$ with a total of p coil positions.
2. Using the stepping mode coil rotation, coil positions are linear sequenced from 0 to $2\pi(p-1)/p$ with $2\pi/p$ interval.
3. At each coil position $coil_n$, using the golden angle method, N spokes were sampled in the k-space domain with the total spokes $N_{total} = N*p \le N_y$, where $N, p \in \mathbb{Z}_+$ (i.e. $p=15$, $N=26$ and $N_y = 401$).
4. m random positions were selected for each data bin $\tilde{d}_l$, and a total of R bins are constructed with non-repeating combination, where $\tilde{d}_l \in \mathbb{C}^{mNx\times 1}$ and $l=1,...,R$.
5. Form the k-t bin matrix $\tilde{d}=[\tilde{d}_1...\tilde{d}_R]$, where $\tilde{d} \in \mathbb{C}^{mNx\times R,}$ and $d_1,...,d_R$ are the column vectors.

The collected k-space data $\mathrm{K} \in \{d_1,...,d_p\}$ can be put into the bin pool, and m non-overlapping positions with the attached k-space data are drawn for each bin $\tilde{d}_l = \Psi_l \mathrm{K}$, where Ψ_l is the corresponding diagonal matrix with a binary mask to extract the required spokes/column k in K. With m positions per bin, the maximum number of non-repeated bins can be formed with $R_{\max} = \frac{p!}{m!(p-m)!}$. Therefore, in the case when $m=2$ and $p=15$, the maximum number of non-overlapping feasible bins is $R_{\max}=105$.

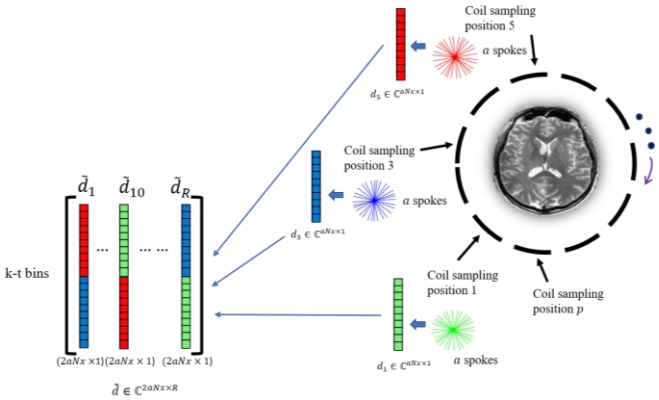

Fig. 1: The k-t bin formation process from the full k-space data matrix in the proposed algorithm. Coil sampling position is at point p. Each k-t bin $\tilde{d}_l$ contains the spokes from $m=2$ different coil positions, and R non-repeated combinations are chosen to form to the k-t bin matrix.

In the proposed k-t sparse bin method, the constructed k-t bin matrix $\tilde{d}$ consists of R sets of m-angle-paired k-space data, and each set can be seen as one under-sampled k-space from one virtual coil. R virtual coils are resembled from the collected k-space. This enables the RRFC system to effectively expand from the p sampling positions to R virtual coils. The less dynamic low-rank matrix L can be calculated using the method of principal component pursuit.

Since the frequency components of the coil sensitivity are mainly low-frequency, whist in the image domain, the sensitivity profile can be compressed with a few dominant eigenvectors. These weighting-like effects from the coil sensitivities have mixed with the original images during signal sampling, along with other system noises. K-space data with different coil sensitivity weightings are randomly recombined to construct data bin $\tilde{d}$, resulting from an averaging effect to all the coil sensitivities during the image reconstruction process. In this way, the coil sensitivity mapping and the time-consuming B1 shimming can be skipped from the scan setup.

Alternatively, we can consider this averaging feature as the global sensitivity map S_{global} from all virtual coils at all sampling positions, and every single local sensitivity map $S_{local} \subset S_{global}$ and the redundancies will be removed during the image reconstruction.

C. Simulation environment

RF coil simulation was performed for single-channel RRFC and multi-channel RRFCA, and all reconstruction were processed in MATLAB 2020b (Mathworks Inc. Natick, MA, USA). The Michigan Image Reconstruction Toolbox [11] was used for the non-uniformed Fourier transform operation for the matrix partition and inversion acceleration. Fig.2 shows the B_1^+ and B_1^- profiles of a dipole coil at 7T (300 MHz), which was modelled using a commercially available electromagnetic simulation package, FEKO (EMSS, SA). The dipole coil has a length of 250mm, and the B field at center slice was used for the imaging. In the first part of the numerical simulation, the Shepp-Logan image was used. A human head-sized homogeneous phantom (Ø: 200 mm) with the relative permittivity of 55 and conductivity of 0.5 s/m was used in the second part of the numerical simulation.

Table I lists the sampling scheme used to generate the k-space data with various coil sampling positions for the proposed method. With every sampling coil position, the maximum number of k-t bins for the image reconstruction is also listed. The coil rotating positions were linearly incremented with the same interval between two consecutive sampling positions. In each simulation, a circle of 2π radian rotation was completed around the scanning object to ensure a widened virtual coil sensitivity distribution.

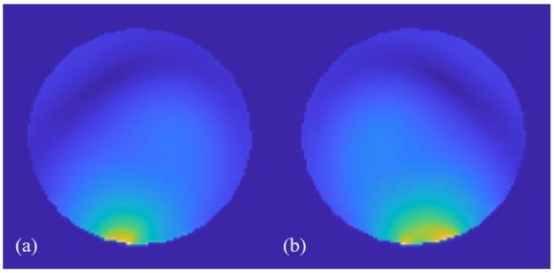

Fig. 2: The coil profile used in the simulations. (a) and (b) are the B_1^+ and B_1^- fields for the dipole coil, respectively.

TABLE I. SIMULATION SCHEME

Sampling positions	Spokes/ position	Sampling points on each radial spoke	Number of radial spokes	Max number of k-t bins	Total spoke number
10	40	256	400	45	3600
15	26	256	390	105	5460
20	20	256	400	190	7600

This simulation setting is used in both Shepp-Logan and Brain numerical simulation

III. RESULTS

A. RRFC reconstruction

The image reconstruction of the Shepp-Logan phantom is shown in Fig. 3, and the brain image reconstruction is shown in Fig. 4. From the difference maps, it is evident that fewer reconstruction errors are found with 20 sampling positions than the ones with 15 and 10 positions. This is because the maximum number of the constructed k-t bins increases with the increased sampling positions. Therefore, the scale of the matrix $\tilde{d}$ enlarges with more image spatial characteristics available for the algorithm to recover the low-rank representation of the original image. In this iterative convex optimization method, the eigenvalue thresholding operation in the low-rank regularization term and soft-thresholding operation in the sparse regularization term can effectively suppress the streaking artefacts introduced by the coil rotation.

B. RRFCA reconstruction

As shown in Fig. 5, using the proposed reconstruction method, much-reduced reconstruction errors are found for the four-element RRFCA than that of the four-element stationary coil array. Hence, the proposed method provides the opportunity to improve the reconstruction quality by utilizing the global coil sensitivity spatial distributions around the object through coil rotation.

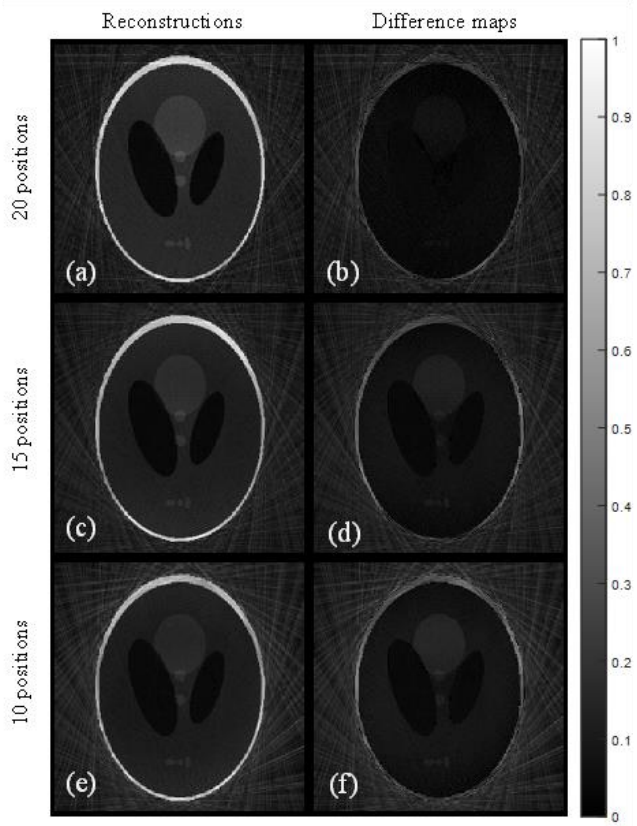

Fig. 3: Reconstruction results and difference maps of a Shepp-logan phantom with the single-element RRFC. (a), (c) and (e) are the reconstructed images with 10, 15 and 20 sampling positions, respectively, and (b), (d) and (f) are the corresponding difference maps.

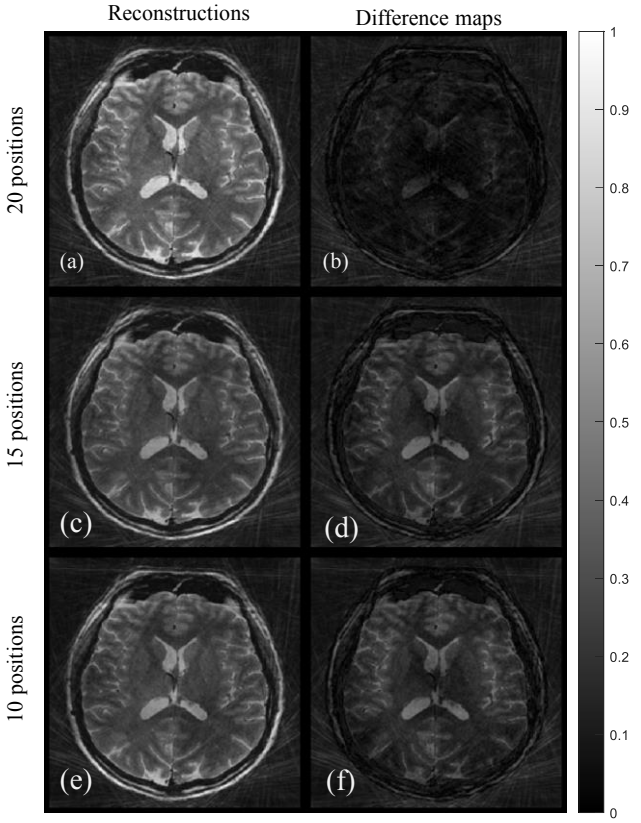

Fig. 4: Reconstruction results and difference maps of the brain image with the single-element RRFC. (a), (c) and (e) are the reconstructed images with 10, 15 and 20 sampling positions, respectively, and (b), (d) and (f) are the corresponding difference maps.

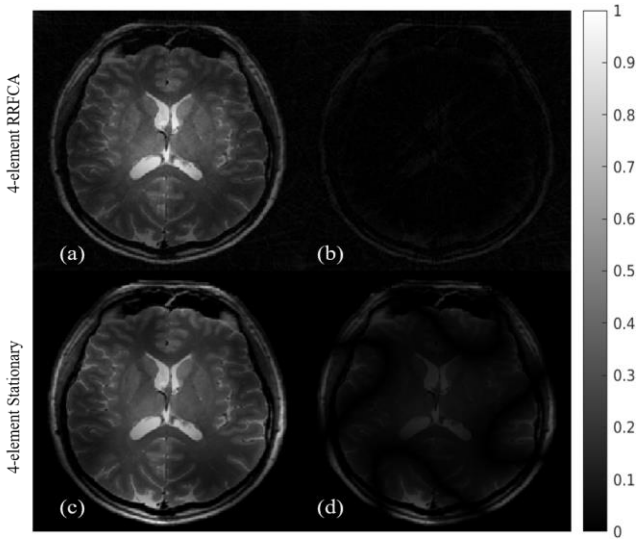

Fig. 5: Image reconstruction comparison between the 4-element RRFCA and a conventional four-element stationary coil array. (a) and (c) are the images reconstructed with the 4-channel RRFCA and the 4-channel stationary array, respectively. (b) and (d) are the corresponding difference maps.

IV. Conclusion

In this paper, we proposed an algorithm based on k-t bin and RPCA for the image reconstruction of the rotating RF coil, which does not require exact coil sensitivity information. The simulation results have proven that the proposed method can successfully recover the image of human-head sized objects at 7T without obvious artefacts. Using a single-coil RRFC, the reconstruction results are comparable to a volume coil. With more coil element, the 4-element rotating coil array outperformed the stationary coil array and the single-element RRFC. In the future, the experiment will be performed to validate the simulation results.

References

[1] M. A. Griswold, S. Kannengiesser, R. M. Heidemann, J. Wang, and P. M. Jakob, "Field-of-view limitations in parallel imaging," *Magnetic Resonance in Medicine: An Official Journal of the International Society for Magnetic Resonance in Medicine,* vol. 52, no. 5, pp. 1118-1126, 2004.

[2] M. Barth, F. Breuer, P. J. Koopmans, D. G. Norris, and B. A. Poser, "Simultaneous multi-slice (SMS) imaging techniques," *Magnetic resonance in medicine*, vol. 75, no. 1, pp. 63-81, 2016.

[3] J. A. Fessler, "Optimization methods for MR image reconstruction," arXiv preprint arXiv:1903.03510, 2019.

[4] A. Trakic et al., "Image reconstructions with the rotating RF coil," *Journal of Magnetic Resonance*, vol. 201, no. 2, pp. 186-198, 2009.

[5] A. Trakic, B. K. Li, E. Weber, H. Wang, S. Wilson, and S. Crozier, "A rapidly rotating RF coil for MRI," *Concepts in Magnetic Resonance Part B: Magnetic Resonance Engineering*, vol. 35B, no. 2, pp. 59-66, 2009.

[6] M. Li et al., "Radial magnetic resonance imaging (MRI) using a rotating radiofrequency (RF) coil at 9.4 T," *NMR Biomed*, vol. 31, no. 2, Feb 2018.

[7] J. Jin et al., "Image Reconstruction for a Rotating Radiofrequency Coil (RRFC) Using Self-Calibrated Sensitivity From Radial Sampling," *IEEE Transactions on Biomedical Engineering*, vol. 64, no. 2, pp. 274-283, 2017.

[8] K. P. Pruessmann, M. Weiger, M. B. Scheidegger, and P. Boesiger, "SENSE: Sensitivity encoding for fast MRI," *Magnetic Resonance in Medicine*, vol. 42, no. 5, pp. 952-962, 1999.

[9] E. J. Candès, X. Li, Y. Ma, and J. Wright, "Robust principal component analysis?," Journal of the ACM (JACM), vol. 58, no. 3, pp. 1-37, 2011.

[10] B. Trémoulhéac, N. Dikaios, D. Atkinson, and S. R. Arridge, "Dynamic MR Image Reconstruction–Separation From Undersampled (k, t)-Space via Low-Rank Plus Sparse Prior," *IEEE transactions on medical imaging*, vol. 33, no. 8, pp. 1689-1701, 2014.

[11] Jeffrey A Fessler, "Michigan Image Reconstruction Toolbox," available at [https://web.eecs.umich.edu/~fessler/code/mri.htm], downloaded [25/02/2020]